Analytical Methods

Accepted Manuscript

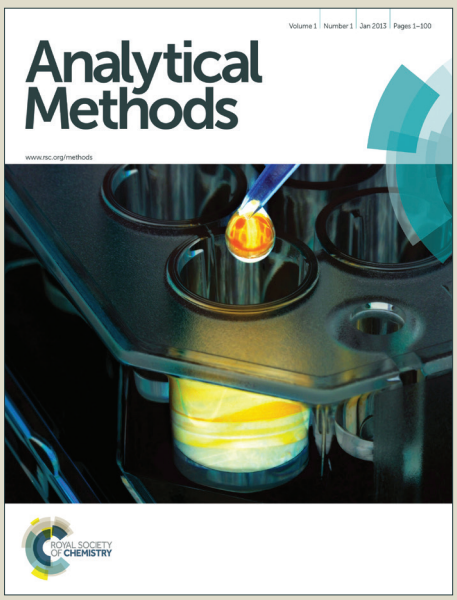

ROYAL SOCIETY OF CHEMISTRY

www.rsc.org/methods

Evaluation of hydrodynamic chromatography coupled with inductively coupled plasma mass spectrometry detector for analysis of colloids in environmental media – Effects of colloids composition, coating and shape

A. Philippe[+], M. Gangloff[+], D. Rakcheev[+], G. E. Schaumann[+]*

[+]Institute for Environmental Sciences, Group of Environmental and Soil Chemistry, University Koblenz-Landau, Landau, Germany

Table of contents

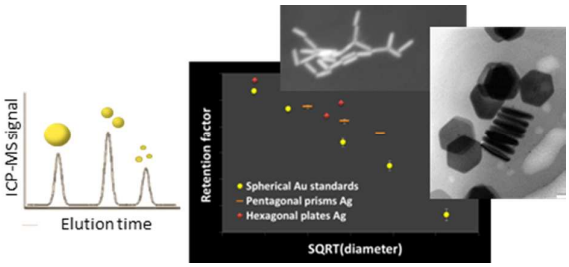

Evaluation of hydrodynamic chromatography coupled with inductively coupled plasma mass spectrometry detector for analysis of colloids in environmental media – Effects of colloids composition, coating and shape

A. Philippe[+], M. Gangloff[+], D. Rakcheev[+], G. E. Schaumann[+]*

[+]Institute for Environmental Sciences, Group of Environmental and Soil Chemistry, University Koblenz-Landau, Landau, Germany

*Email address: schaumann@uni-landau.de

Abstract

In this study, we evaluated hydrodynamic chromatography (HDC) coupled with inductively coupled plasma mass spectrometry (ICP-MS) for the analysis of nanoparticles with different coating and shapes. Using two commercially available HDC columns (Polymer Labs-PDSA type 1 and 2) and a set of well characterised calibrants of different materials ($Au^{(0)}$, $Ag^{(0)}$, SiO_2, polystyrene), coatings (citric acid and tannic acid), and shapes (spheres, rod-like prisms, and hexagonal plates) we demonstrated that temperature does not influence the size resolution and, therefore, can be adapted to the sample particularity. Retention behaviour was not influenced by the particle material. However, a minor influence of the particle coating was observed for tannic acid coated silver nanoparticles. Particle shape noticeably affects the retention behaviour and can lead to erroneous size estimation if spherical calibrants are used to determine their effective diameter. Using the ICP-MS detector in the single-particle modus made possible to discriminate between spherical and rod-like particles despite some limitations. However, the development of a comprehensive physical model for the elution behaviour of particles with complex shapes in HDC is needed for obtaining quantitative information about the shape using HDC. Our findings demonstrate that HDC-ICP-MS is a promising method for measuring the size and the concentration of spherical inorganic colloids in complex media and suggest that HDC may be increasingly implemented in environmental science.

Keywords: hydrodynamic chromatography, ICP-MS, single particle ICP-MS, nanoparticles, colloids, gold, silver, silica, shape.

Introduction

The growing scientific interest for natural and engineered colloids in the environment has pinpointed the lack of suitable methods for characterising colloids in environmental samples[1–4]. The most important parameters of colloidal suspensions to be obtained are size, elemental composition, concentration, structure, charge, and coating of the colloids, which require dedicated techniques[2]. In environmental matrices, inorganic ions, natural organic matter (NOM), living organisms, and inorganic particles can interact with colloids[5]. An ideal detection and characterisation technique should therefore additionally distinguish the targeted particles from the natural colloids, and remain accurate at realistic concentrations (ng L^{-1})[3,6].

In the analytical toolbox dedicated to colloid characterization, hydrodynamic chromatography (HDC) is one of the most promising techniques as it provides reliable size separation that is largely independent of the matrix[7–9].The separation mechanism is based on different samplings of the flow velocity profile due to differences in the effective diameter[10]. One important advantage of HDC over other size separation techniques like size exclusion chromatography or field flow fractionation is its high flexibility and robustness. Indeed, size separation efficiency is widely independent of flow rate, eluent composition, and surface charge[7,11]. For inorganic colloids, element specificity and the low detection limit (in the ng L^{-1} range for most elements) of an ICP-MS detector can complement the flexibility of HDC. This hyphenated technique was applied successfully to environmental samples[7–9] and the simultaneous determination of size and concentration of colloids suspended in complex media using HDC-ICP-MS has been reported[7].

The average effective diameter of an unknown suspension can be estimated with HDC by using a calibration curve obtained with well-characterized calibrants. However, the universality of this calibration curve has not yet been fully demonstrated although HDC is applied to diverse particle types. Indeed, the effect of particle density and shape remained unaddressed. In addition, an effect of particle coating was observed for gold nanoparticles but is still not well understood[12], although it has already been reported that the retention factor in HDC is independent of the surface charge of the particles[13].

Non-spherical particles are common in nature. Colloids like clays[14] and microorganisms[15] can have plate- and rod-like shapes. Engineered nanoparticles with various shapes can be routinely synthesized[16,17]. In addition, a portion of colloids present in the environment may be homo- or heteroagglomerated[18] and form complex fractal structures[19]. Therefore, it is crucial to understand the effect of the particle shape and morphology on the elution behaviour in HDC for the analysis of environmental samples.

In this study we investigated the effect of temperature, density, coating, and shape of well characterised standard particles on their elution behaviour in HDC in order to explore the limits of a universal size calibration. Furthermore, we took advantage of the single particle mode of the ICP-MS to extend the analytical possibilities of HDC-ICP-MS for non-spherical particles.

Material and methods

Reference colloids

Standard citrate-stabilised gold nanoparticles (Aldrich, Germany) were used as size calibrants with the ICP-MS detector. The core and hydrodynamic diameters of the gold particles were examined using SEM and NTA, respectively; these data are available elsewhere[20]. Certified analytical polystyrene standard particles (nominal diameter: 50, 100, 200, 300, and 500 nm) were provided by Beckmann-Coulter. Spherical silver nanoparticles stabilised with citric or tannic acid and silica particles were purchased from Nanocomposix, while non-spherical silver nanoparticles were purchased from Sciventions.

HDC-ICP-MS-system

Devices and methods were similar to those reported elsewhere[20]. The eluent was Milli-Q water (MQW, resistivity = 18 M□□cm) containing 0.536 g L^{-1} (2 mM) $Na_2PO_4.7H_2O$ (Aldrich, purity > 99%), 0.5% w/w (60 mM) formaldehyde solution (Alfa Aesar, 37% w/w H_2O, 7–8% MeOH), 0.5 g L^{-1} (1.8 mM) sodium dodecyl sulphate (Alfa Aesar), 1 g L^{-1} (3.2 mM) Brij L23 (Alfa Aesar) and 1 g L^{-1} (3.2 mM) Triton X-100 (Alfa Aesar). The pH value of the eluent was in all cases between 7.5 and 8. As Ba^{2+} was present as trace impurity in the eluent, it was used as time marker. A PL-PSDA type 2

column (Agilent, Germany, separation range: 20-1200 nm) was used for the investigation of temperature, coating, and density effects with a flow rate of 2.1 mL min^{-1}, while a PL-PSDA type 1 column (Agilent, Germany, separation range: 5-300 nm) was used for measuring non-spherical particles at a flow rate of 1.7 mL min^{-1} unless otherwise stated. The injection volume was 30 µL for all of the samples measured in normal mode ICP-MS. For studying the effect of temperature, the HDC-column was thermostated using a water bath connected to a thermostat. While $Ag^{(0)}$ and $Au^{(0)}$ particles were detected using ICP-MS, a UV-visible-detector was used at an absorption wavelength of 200 nm to detect SiO_2 and polystyrene particles.

In single particle-ICP-MS mode, elution rate was 1.7 mL min^{-1} during 6.17 min and decreased over 30 s to 0.5 mL min^{-1} until the end of the elution. In this way, detection of single particle was optimized. Separation efficiency is only weakly influenced by changes in flow rate[7]. Particle concentrations were within the range 10-100 µg L^{-1}. The injection volume was adjusted for each sample for optimizing the number of single particle detected per injection. Dwell time of the ICP-MS detector was 5 ms. Data were analyzed using an Excel-macro designed to remove the background signal and aberrant values and described elsewhere[20]. The citrate stabilized silver nanoparticles were used as calibrants to determine the diameter of a hypothetical compact sphere having the same mass as the detected particles from the height of spike signals.

Nanotracking analysis and dynamic light scattering

Nanotracking analyses were carried out with a LM20 (Nanosight) analyser following a standard procedure[21]. Confidence intervals were calculated from four measurements.

A Delsa Nano C particle analyser from Beckmann-Coulter (laser wavelength: 658 nm, scattering angle: 165°, temperature: 20 °C) was used for the light scattering measurements. Z-average hydrodynamic diameter was calculated using the CONTIN method[22]. Measure position was 6.15 mm above the bottom of the vials. Polystyrene cuvettes were used. The stable suspensions were measured three times over 60 seconds accumulation time.

Scanning and transmission electron microscopy

A Quanta250 (FEI) scanning electron microscope (SEM) equipped with an X-ray diffraction system (Quantax; Bruker) was used for the microscopic characterisation of the colloid standards. 1 µL of the dispersion was deposited on an aluminium support covered by a carbon tape and dried in the air for 15 minutes. Samples were then directly analysed under high vacuum using the Everhart Thornley detector for particles larger than 100 nm or the backscattered electrons detector for particles smaller than 100 nm. The elemental composition of the particles was verified by X-ray analysis. At least 140 primary particles were measured per sample.

A LEO 922 OMEGA transmission electron microscope (200 kV; Carl-Zeiss) was used for characterization of length and thickness of the silver nanoparticles having the shape of hexagonal plates. 5 µL of the nanoparticles stock suspension were placed onto an ultrasound nebulizer (proprietary system developed at the Karlsruhe Institute for Technology). After nebulisation onto a copper grid covered with a polymeric layer, the specimens were placed into a sample holder. Measurements were carried out under deep freezing (liquid nitrogen). Length and thickness of at least 300 primary particles were measured for each suspension.

Results and discussion

Characterization of standard suspensions

Table 1 summarizes characteristics of spherical standard particles used in this study obtained with SEM, NTA and DLS. The spherical shape of these standards was confirmed using SEM. Differences between the sizes obtained using different methods were expected and observed. While number average core diameters were computed from SEM results, number average and intensity weighted average hydrodynamic diameters are obtained with NTA and DLS, respectively[21,22]. Therefore, it is expectable that size values obtained using DLS are higher than those with NTA and SEM as we observed. Except for 40 nm citrate stabilized silver nanoparticles, the values obtained with SEM and NTA were in the range of the confidence intervals, indicating that, in these cases, hydrodynamic diameter and core diameter are comparable.

Table 1: Mean characteristics of standard spherical particles used in this study. The errors given correspond to the confidence intervals at 95% calculated using 4 replicates. For SEM measurements, standard deviations of the size distributions are given into brackets. n.m. means "not measured": particles smaller than 30 nm were not detectable neither with SEM nor with NTA.

Particle type	Nominal size in nm	Core diameter in nm (SEM)	Hydrodynamic diameter in nm (NTA)	Hydrodynamic diameter in nm (DLS)
Ag citrate stabilised	20	n.m.	n.m.	28 ± 1
	40	40 (4)	51 ± 3	55 ± 1
	80	82 (5)	79 ± 6	93 ± 2
	100	100 (6)	98 ± 6	112 ± 9
Ag tannate stabilised	20	n.m.	n.m.	27 ± 2
	40	40 (3)	44 ± 3	49 ± 5
	80	82 (5)	82 ± 3	84 ± 4
	100	102 (12)	94 ± 6	96 ± 5
SiO_2	80	86 (6)	85 ± 8	101 ± 2
	120	122 (7)	118 ± 8	137 ± 4
	200	212 (13)	187 ± 6	220 ± 11

Non-spherical particles were characterized using the same methods, except for the hexagonal plates, which were measured using a TEM instead of a SEM since the resolution of our SEM was too low for determining the thickness of these particles (around 10 nm). Representative SEM and TEM pictures of pentagonal prisms and hexagonal plates can be found in the supporting information (**figures S1 and S2**). The results obtained using NTA and DLS are not easily interpretable as computation of the sizes are based on the assumption that particles are spherical in both methods[21,22]. Contrary to the results obtained with spherical particles, the hydrodynamic diameters measured by NTA and DLS were lower than the effective diameters (longest distance between two points of the particle) obtained from microscopy (**table 2**). These discrepancies increase with the average aspect ratios (ratio of length to broadness) of the corresponding suspensions (**table 2**). The values obtained by NTA were higher than the values obtained by DLS in contrast to the observation made for spherical particles. NTA values were also nearer to the effective diameters than DLS values, indicating that NTA is less influenced by

the particles shape than DLS. Both NTA and DLS use the Stokes-Einstein equation to compute hydrodynamic diameter from the diffusion coefficient[21,22]. As this equation is valid only for spherical particle, the calculation of the hydrodynamic diameter is biased for other shapes. Results obtained using DLS are additionally biased by the effect of particle geometry on the light scattering intensity[22], explaining the high bias of DLS compared to NTA.

The TEM pictures of hexagonal plates (**figure S2**) show the presence of particles smaller than 10 nm in addition to the expected particles. The small particles could be detected and resolved from the larger particles with HDC-ICP-MS. It was hence possible to analyse large shaped particles while ignoring those small particles. The detection limit of our NTA device for the size is about 30 nm for silver. NTA measurements were therefore not affected by the presence of those impurities. However, DLS may be influenced by those impurities.

Table 2: Characterisation of the standard non-spherical particles used in this study. Confidence intervals at 95% were calculated using at least 4 replicates. Effective diameters (longest distance between two points of the particle) were calculated using the average lengths and broadness's measured with electron microscopes. Aspect ratios denote the ratio of length to broadness. For microscopy measurements, standard deviations of the size distributions are given into brackets.

Particle type	Nominal length in nm	Length in nm (SEM/TEM)	Broadness in nm (SEM/TEM)	Effective diameter in nm	Aspect ratio	Hydrodynamic diameter in nm (NTA)	Hydrodynamic diameter in nm (DLS)
Ag pentagonal prisms	70	56 (7)	31 (4)	64	1.81	61 ± 0	51 ± 2
	118	91 (11)	35 (6)	97	2.60	67 ± 1	32 ± 1
	165	131 (16)	35 (5)	136	3.74	86 ± 3	38 ± 1
Ag hexagonal plates	60	29 (3)	8 (1)	30	3.63	30 ± 6	31 ± 3
	80	79 (5)	14 (4)	80	5.64	62 ± 2	47 ± 2
	110	92 (1)	10 (1)	93	9.20	58 ± 1	42 ± 2

Effect of the temperature

In order to investigate the effect of temperature on the colloid elution, the retention factors of five gold calibrants (nominal diameters: 30, 50, 100, 150, and 250 nm) were determined using a HDC column thermostated at: 10.3±0.1°C, 20.3± 0.1°C and 34.8±0.1°C, respectively. For each suspension the retention factors remained constant over the range of studied temperatures indicating that the elution behaviour is independent of the temperature (**figure 1**). Therefore, temperature is certainly a negligible factor in HDC and can be adjusted to the sample specificity. For instance, performing measurements at low temperatures could contribute to minimizing possible alterations of the particles (oxidation, dissolution, etc.) throughout the elution and, thus, reducing measurement artefacts. In addition, these data confirm that enthalpic effects can be neglected in HDC.

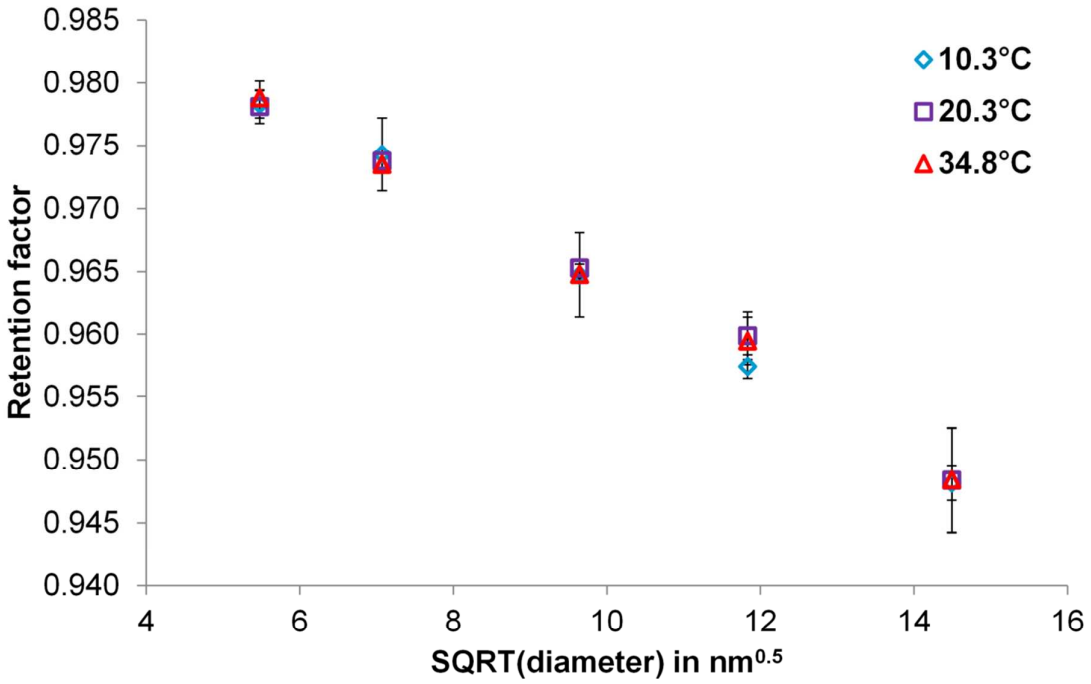

Figure 1: Retention factors of gold nanoparticles measured using HDC-ICP-MS plotted against the square root of the mean diameter. The HDC column was thermostated at three different temperatures. The error bars represent the confidence intervals at 95% calculated using three replicates.

Density effect

It is necessary to know the effect of particle density on the retention behaviour in order to ensure that dense colloids, like gold nanoparticles for instance, can be used as universal calibrants. Therefore, retention factors of particles with different size and composition were measured with HDC-UV-ICP-MS. We chose $Au^{(0)}$, $Ag^{(0)}$, SiO_2, and polystyrene particles revealing contrasting densities of 19.32 $g.cm^{-3}$, 10.49 $g.cm^{-3}$, 2.19-2.66 $g.cm^{-3}$, and 1.04 $g.cm^{-3}$, respectively. The calibration curves obtained by plotting the retention factors over the square root of the diameters are superimposed on each other (**figure 2**) indicating that bulk density and, even more generally, particle bulk composition does not influence the retention factor in HDC. This demonstrates the applicability of universal calibrants for sizing spherical colloids. This is an excepted outcome as the diffusion coefficient of colloids is not expected to significantly change with the density. Therefore, the particles will be able to sample fast enough the streamlines in the HDC-column independently of the density[10].

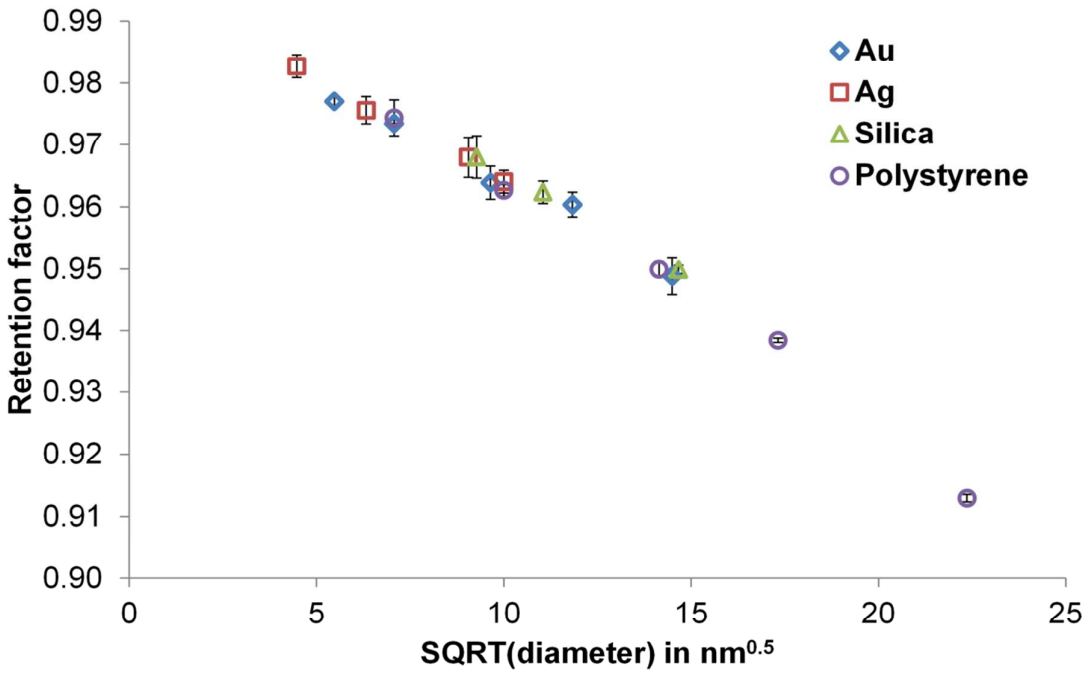

Figure 2: Retention factors of standard citrate stabilised gold and silver colloids, bare silica, and polystyrene colloids measured using HDC-UV-ICP-MS (column type 2) plotted against the square root of the mean diameter. The error bars represent the confidence intervals at 95% calculated using three replicates.

Effect of particle coating on elution behaviour

Most colloids present in environmental media are expected to be coated by natural organic matter and inorganic ions[23,24]. In order to determine the size of unknown colloids in natural water, it is necessary to test the universality of the calibration in dependence of particle coating. For this, the retention factors of $Ag^{(0)}$ nanoparticles with two different coatings, citric acid and tannic acid, were measured with HDC-ICP-MS. Tannic acid was chosen for its structural similarities with some humic substances[25]. Tannic acid coated nanoparticles tend to elute slightly slower than expected from their sizes (**figure 3**). Differences in retention factors between citrate coated and tannate coated particles with a mean diameter of 20 nm, 40 nm, and 80 nm are inside the confidence intervals at 95%, while for particles with a mean diameter of 100 nm, it differs clearly (**figure 3**). The resulting discrepancies between the sizes determined due to the coatings are in the range 8-22 nm, whereas the size determination error due to the measurement uncertainty is in the range 0.1-22 nm. A weak affinity due to π-π interactions between the column packing (polystyrene) and the electron-donating groups of tannic acid molecules may explain the effect of the coating. This would also explain why larger particles are more influenced by the coating than smaller ones; because the surface available for interaction with the packing material increases with size. This affinity could be reduced by using packing material with lower affinity or by using a capillary instead of a packed column[26].

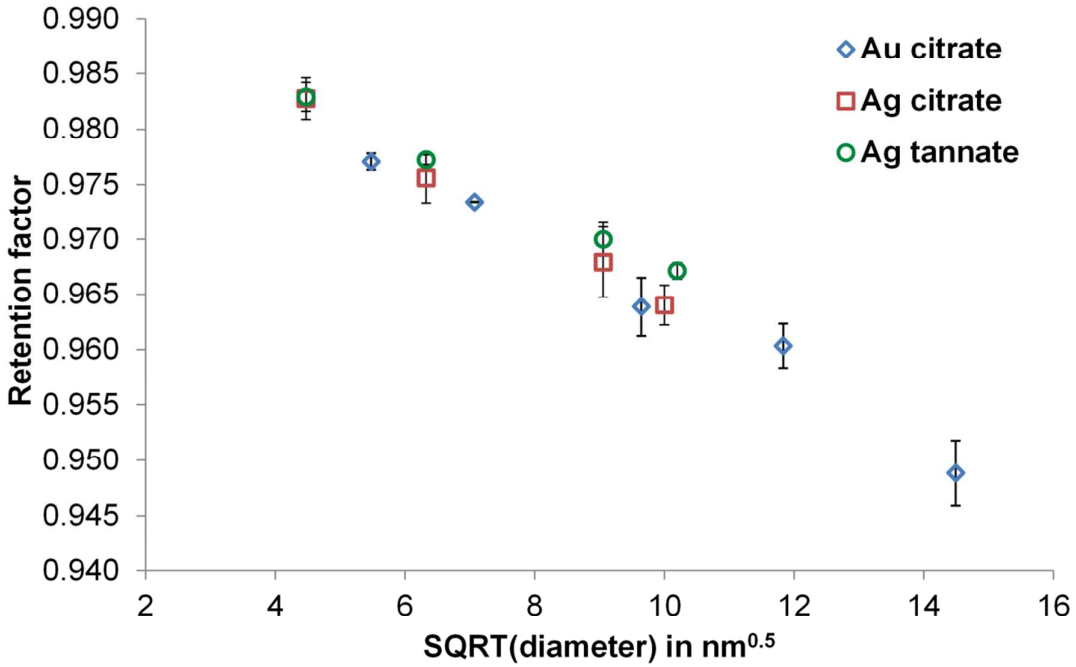

Figure 3: Retention factors of standard citrate stabilised gold and silver colloids and tannate stabilised silver colloids measured using HDC-ICP-MS (column type 2) plotted against the square root of the mean diameter. The error bars represent the confidence intervals at 95% calculated using three replicates.

These findings seem to contradict results reported by Gray *et al*. [12], who observed major differences between retention factors of citrate- and tannate-coated gold nanoparticles measured with HDC-ICP-MS. We explain this apparent contradiction by the differences in eluent composition. Indeed, Gray *et al*. used an eluent with an ionic strength ten times lower than ours and a concentration of surfactant more than two times lower than ours. Indeed, ionic strength is an important factor in HDC[11]. At low ionic strength, the tannic acid molecules may have a more extended conformation on the nanoparticle surface than at high ionic strength and hence they are available to larger extent or chemical interactions with the packing material.

Shape effect

We measured the retention factor of the characterized silver pentagonal prisms and silver hexagonal plates, both assimilated to cylinders, with HDC-ICP-MS with gold spherical standards (**figure 4**). The non-alignment of the retention factors of the non-spherical particles with the spherical standards

indicates a strong effect of the shape on the retention factor. For a particle with a plate-shape or a rod-shape the effective diameter would be strongly underestimated if the spherical gold calibrants would be used as calibrants.

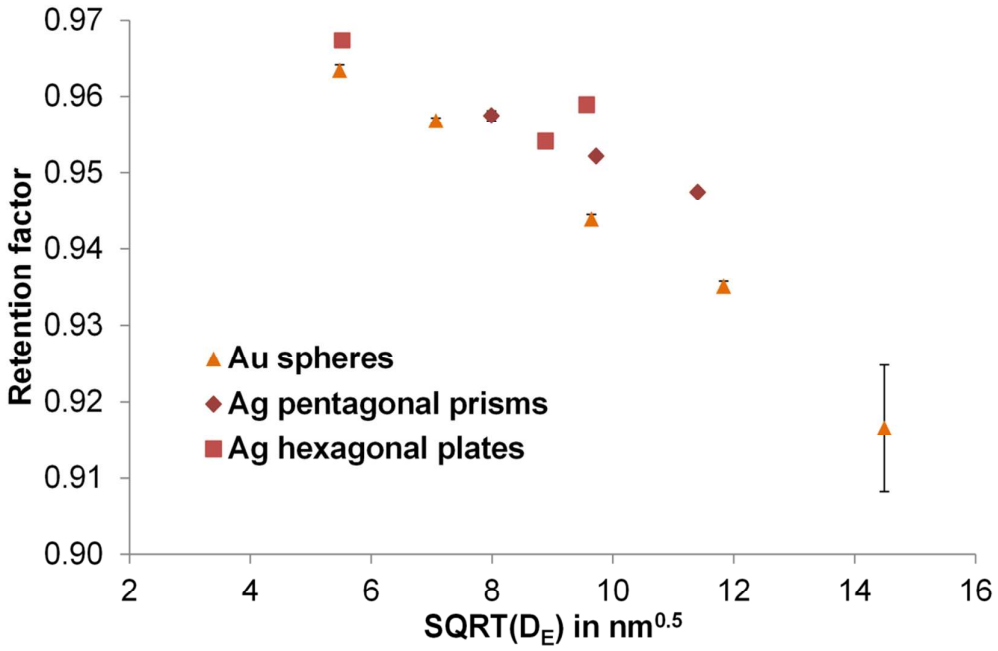

Figure 4: Retention factors of standard spherical gold particles, silver pentagonal prisms, and silver hexagonal plates measured using HDC-ICP-MS (column type 1) plotted against the square root of the mean effective diameter (D_E). The error bars represent the confidence intervals at 95% calculated using three replicates.

The absolute difference between the effective diameter calculated using the retention time in HDC and the effective diameter measured using electron microscopy increases with the aspect ratio of the particle (**figure 5**). This clear relation indicates that the effect of the shape has a geometric and hydrodynamic origin rather than being an effect of affinity of the particles with the packing material of the HDC column. To confirm this hypothesis the same suspensions were measured at different temperature and flow velocities (**table 3**). Affinity effects are expected to increase when the flow rate decreases as analytes have a longer time to interact with the packing material. Increase in temperature also reduces the effect of affinity. No difference between the sizes measured under different elution conditions was observed, except for the suspension HP-80 for which the estimated effective diameter

is even smaller at the highest flow rate and temperature. We can hence conclude that the role of affinity is minor and that it is not responsible for the highly different elution behaviour of spherical and non-spherical particles. We hence conclude from these data that a purely geometric and hydrodynamic effect is responsible for these discrepancies. However, a complete theoretical understanding of this effect requires the development of a physical model for the elution of non-spherical particles. In particular, the retention factor dependency on temperature and flow rate of the dispersion HP-80 cannot be explained by the classical HDC separation mechanism and could result from a different average orientation of these flat particles relative to the streamlines at high flow rates and temperatures. Interestingly, extrapolation of the correlation lines of the aspect ratio and the effect of particle geometry in term of size extrapolation (**figure 5**), indicates that even at an aspect ratio of one, a difference still exists between sphere and non-spherical shape (here prisms). The aspect ratio is hence not the only relevant parameter; the intrinsic shape of the particle is also important for the elution in HDC.

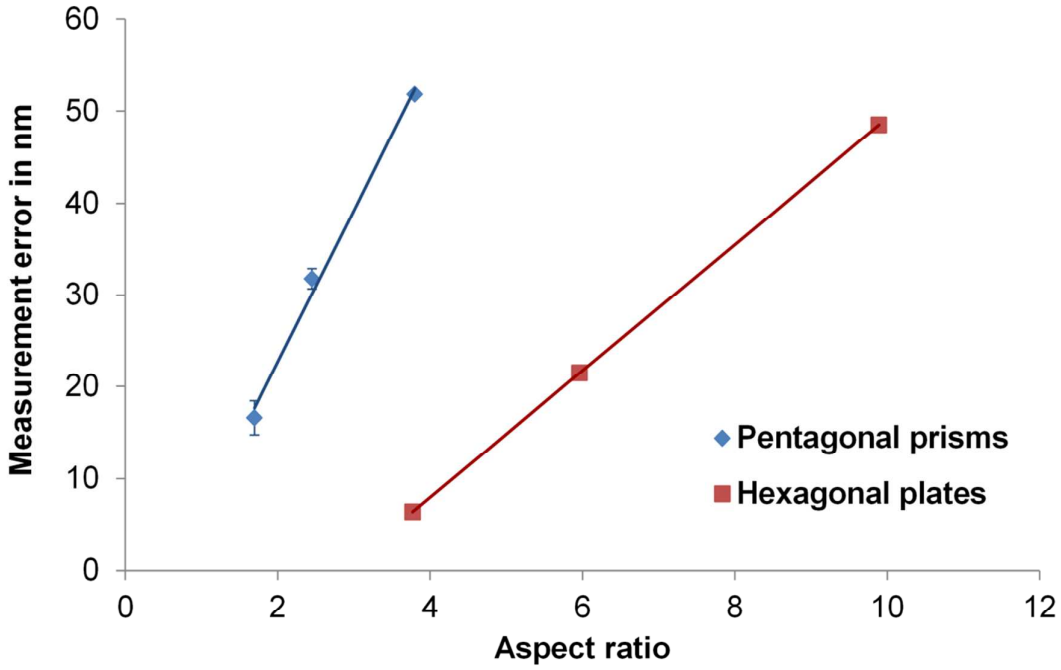

Figure 5: Measurement error function of the aspect ratio of the silver pentagonal prisms (PP) and hexagonal plates (HP). Measurement error is defined as the absolute difference between the average effective diameter measured with TEM and the average effective diameter determined using HDC-ICP-MS, using standard spherical gold nanoparticles as calibrants. The error bars represent the confidence intervals at 95% calculated using three replicates.

Table 3: Effective diameters of silver pentagonal prisms (PP-nominal size) and silver hexagonal plates (HP-nominal size) measured with HDC-ICP-MS at two different flow rates and temperatures. The uncertainties represent the confidence intervals at 95% calculated using three replicates. n.r. means that the peaks of the larger hexagonal plates and the small particles present as impurities were not resolved under these conditions and that retention time could not be measured.

Flow rate (mL min^{-1})	1.70	0.80	2.02
Temperature (°C)	20	20	35
PP-70	47.2 ± 1.8 nm	45.7 ± 3.6 nm	46.0 ± 0.1 nm
PP-118	62.7 ± 1.1 nm	61.2 ± 6.0 nm	62.0 ± 2.3 nm
PP-165	78.2 ± 0.1 nm	85.2 ± 7.8 nm	77.0 ± 0.1 nm
HP-60	24.3 ± 0.7 nm	21.1 ± 1.4 nm	24.8 ± 0.1 nm
HP-80	56.7 ± 2.4 nm	55.7 ± 24.7 nm	43.6 ± 3.4 nm
HP-110	43.4 ± 1.1 nm	n.r.	n.r.

These findings indicate that unless the shape of the sample is known and calibrants with similar aspect ratio are used, there is a possible bias in the size estimation in HDC due to the particle geometry. It is theoretically not possible to discriminate between spherical and non-spherical particles with HDC alone since only one parameter can be determined (retention factor), whereas two parameters (length and broadness) are required to describe a cylinder, for instance. Measuring two relevant parameters simultaneously should thus help in better describing the shape of particles. This is possible using HDC coupled to single particle ICP-MS (SP-ICP-MS)[20].

SP-ICP-MS denotes a mode of the ICP-MS detector in which single particles are detected individually as spike signals[27–29]. When HDC is coupled with SP-ICP-MS spike height and retention time can be collected on a single particle basis[30]. As the spike height is proportional to the particle mass and the effective diameter (D_E) can be computed from retention time, it is possible to distinguish between compact and loose particles as demonstrated for gold nanoparticle agglomerates[20]. A practical way to present such results is to plot the effective diameter over the diameter calculated from the spike height assuming a spherical shape ("core" diameter D_C) for every detected particle.

In order to implement this method to non-spherical particles, the three silver pentagonal prisms suspensions were measured with HDC-SP-ICP-MS. Silver hexagonal plates could not be characterised using HDC-SP-ICP-MS because of the high amount of small particles present as impurities as noted above. Covering of the two particles distributions on the chromatograms hindered the correct analysis of the data. Concerning the pentagonal prisms, between 470 and 1000 particles were detected for each suspension. As example, the $D_E(D_C)$ graph for the pentagonal prisms with nominal length 118 nm is plotted in **figure 6a**. D_E values were highly dispersed due to the intrinsically low size resolution of HDC and hindered the use of a mathematical fitting directly on the data clouds in the $D_E(D_C)$ graph. In order to analyse the tendency of the data clouds, the modes of D_C and D_E distributions were calculated for each suspension (**figure 6b**).

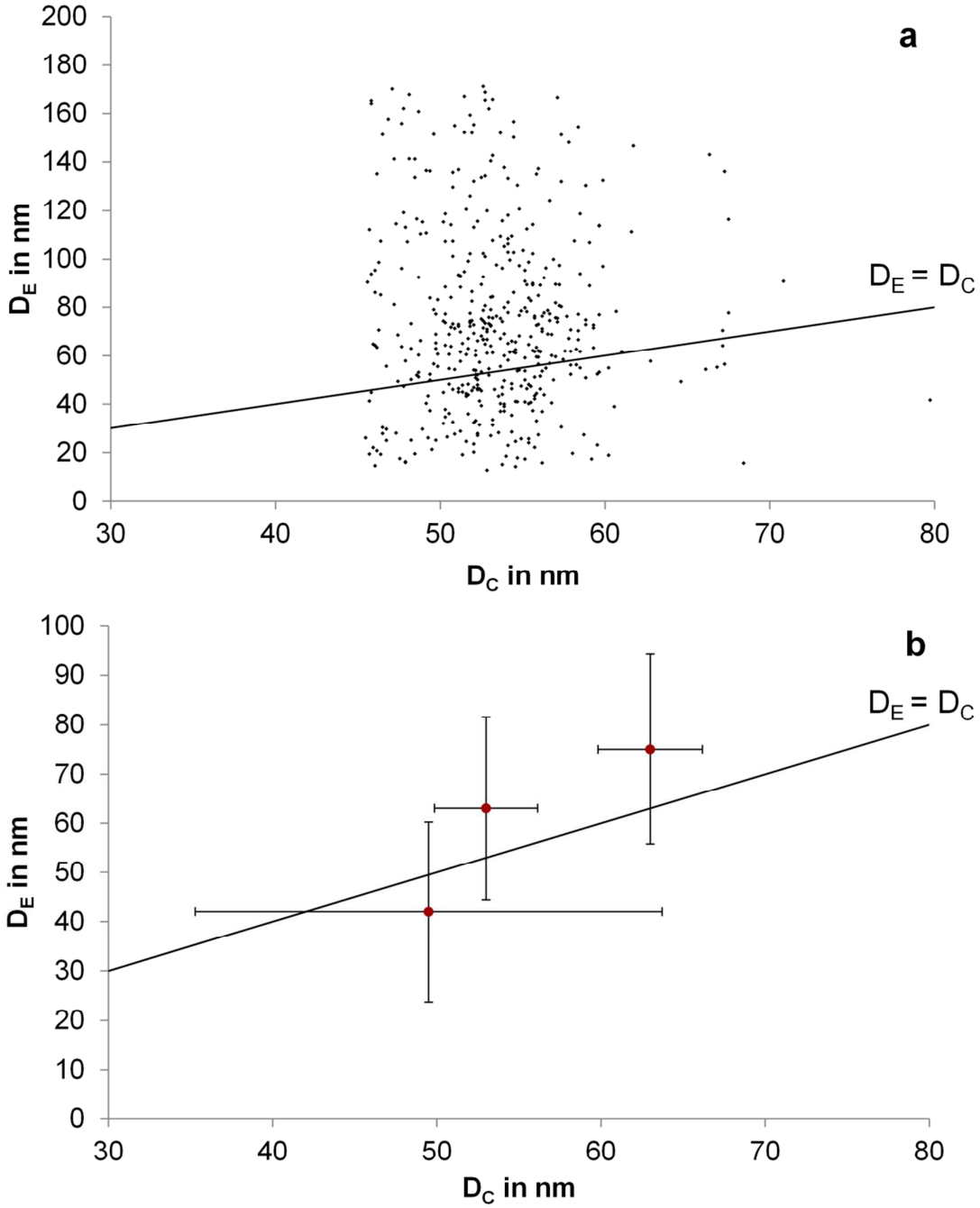

Figure 6a: Effective diameter (D_E) calculated from the retention time over the "core" diameter (D_C) calculated from the spike signal height for the silver pentagonal prisms suspension with nominal diameter 118 nm. 6b: distribution mode of the effective diameter (D_E) calculated from the retention time over the distribution modes of the "core" diameter (D_C) calculated from the spike signal height for the three silver pentagonal prisms suspensions. Bars depict the standard deviation of the corresponding dataset. The straight line corresponds to the function $D_E = D_C$.

The line described by the function $D_E = D_C$ corresponds to that expected for spherical particles for which the two diameters obtained using HDC-SP-ICP-MS should be equal. For non-spherical particles non-linear functions would be expected. Considering that each distribution represents a unique suspension and that the particles have similar shape in each suspension, the three points in **figure 6b** indicate that the particles are not spherical. It has to be noted that D_E measured by HDC do not correspond to a real geometric diameter due to the use of spherical calibrants as discussed above. This explains the observation that, for one suspension, the mode of the D_E is even smaller than the mode of the D_C, which is physically impossible. Nevertheless, the shape of the $D_E(D_C)$ curve gives some indication on the shape of the particles. For monodisperse small non-spherical particles, HDC-SP-ICP-MS cannot distinguish between different shapes unless the size distribution is broad enough for analysing the shape of the curve and the aspect ratio high enough for seeing a clear difference with the $D_E = D_C$ line. For instance, considering the silver pentagonal prisms only the suspensions with the largest sizes (91 and 131 nm) could be efficiently distinguished from spherical particles using HDC-SP-ICP-MS (**figure 6b**). Thus, qualitative, but not quantitative discrimination between spherical and non-spherical particles is possible using HDC-SP-ICP-MS only in such favourable cases.

Conclusion

Our results demonstrate the high flexibility and robustness of HDC in terms of particle properties. This is an advantage over other separation techniques such as field flow fractionation and size exclusion chromatography. Therefore, HDC is a powerful complementary tool to those techniques and can be widely implemented in environmental science. However, the measurement of non-spherical particles is still a challenge since the shape strongly influences the retention behaviour in HDC and other separation techniques. Thus, complications due to particle geometry have to be considered throughout the measurement of unknown particles since it could lead to erroneous conclusions. If the colloid concentration is in the range of mg L^{-1}, it is possible to couple HDC with a multi-angle light scattering online or offline to obtain additional information on the shape[31]. For lower concentrations, using SP-ICP-MS as detection technique can help in distinguishing between spherical and non-spherical particles, provided that the size distribution is large enough and that the analytes are similarly shaped.

The performance of this coupling technique could be improved by using a capillary instead of a packed column[26], as the resolution power is higher in the former case[32]. Coupling HDC with orthogonal techniques as electrophoresis could also help in distinguishing between different particle shapes[32].

Acknowledgments

We kindly acknowledge Mohammad Fotouhi Ardakani from the Karlsruhe Institute of Technology for the TEM measurements and the DFG for financial support within the research unit FOR 1536 INTERNANO, subproject MASK (SCHA849/16).

Supporting information

Electronic supplementary Information (ESI) available: Figure S1 and S2.

References

1. D. J. Burleson, M. D. Driessen, and R. L. Penn, *Journal of Environmental Science and Health, Part A*, 2005, **39**, 2707–2753.

2. M. Hassellöv, J. W. Readman, J. F. Ranville, and K. Tiede, *Ecotoxicology*, 2008, **17**, 344–361.

3. B. M. Simonet and M. Valcárcel, *Analytical and Bioanalytical Chemistry*, 2009, **393**, 17–21.

4. K. Tiede, A. Boxall, S. Tear, J. Lewis, H. David, and M. Hassellov, *Food Additives and Contaminants*, 2008, **25**, 795–821.

5. G. R. Aiken, H. Hsu-Kim, and J. N. Ryan, *Environmental Science & Technology*, 2011, **45**, 3196–3201.

6. B. Nowack, J. F. Ranville, S. Diamond, J. A. Gallego-Urrea, C. Metcalfe, J. Rose, N. Horne, A. A. Koelmans, and S. J. Klaine, *Environmental Toxicology and Chemistry*, 2012, **31**, 50–59.

7. A. Philippe and G. E. Schaumann, *PLoS ONE*, 2014, **9**, e90559.

8. K. Tiede, A. B. Boxall, D. Tiede, S. P. Tear, H. David, and J. Lewis, *Journal of Analytical Atomic Spectrometry*, 2009, **24**, 964–972.

9. K. Tiede, A. B. Boxall, X. Wang, D. Gore, D. Tiede, M. Baxter, H. David, S. P. Tear, and J. Lewis, *Journal of Analytical Atomic Spectrometry*, 2010, **25**, 1149–1154.

10. A. M. Striegel and A. K. Brewer, *Annual Review of Analytical Chemistry*, 2012, **5**, 15–34.

11. H. Small, F. L. Saunders, and J. Solc, *Advances in Colloids and Interface Science*, 1976, **6**, 237–266.

12. E. P. Gray, T. A. Bruton, C. P. Higgins, R. U. Halden, P. Westerhoff, and J. F. Ranville, *Journal of Analytical Atomic Spectrometry*, 2012, **27**, 1532–1539.

13. D. C. Prieve and P. M. Hoysan, *Journal of Colloid and Interface Science*, 1978, **64**, 201–213.

14. Y. Furukawa, J. L. Watkins, J. Kim, K. J. Curry, and R. H. Bennett, *Geochemical transactions*, 2009, **10**, 11.

15. D. A. Bazylinski and R. B. Frankel, *Nature Reviews Microbiology*, 2004, **2**, 217–230.

16. N. Cathcart and V. Kitaev, *ACS nano*, 2011, **5**, 7411–7425.

17. W. Liu, W. Sun, A. G. L. Borthwick, and J. Ni, *Colloids and Surfaces A: Physicochemical and Engineering Aspects*, 2013, **434**, 319–328.

18. E. M. Hotze, T. Phenrat, and G. V. Lowry, *Journal of Environmental Quality*, 2010, **39**, 1909–1924.

19. R. Amal, J. A. Raper, and T. D. Waite, *Journal of Colloid and Interface Science*, 1990, **140**, 158–168.

20. D. Rakcheev, A. Philippe, and G. E. Schaumann, *Analytical Chemistry*, 2013, **85**, 10643–10647.

21. V. Filipe, A. Hawe, and W. Jiskoot, *Pharmaceutical Research*, 2010, **27**, 796–810.

22. R. Finsy, *Advances in Colloids and Interface Science*, 1994, **52**, 79–143.

23. R. Beckett and N. P. Le, *Colloids and Surfaces*, 1990, **44**, 35–49.

24. K. Hunter and P. Liss, *Limnology and Oceanography*, 1982, 322–335.

25. A. Nebbioso and A. Piccolo, *Analytical and Bioanalytical Chemistry*, 2013, **405**, 109–124.

26. J. G. DosRamos and C. A. Silebi, *Journal of Colloid and Interface Science*, 1990, **135**, 165–177.

27. D. M. Mitrano, E. K. Lesher, A. Bednar, J. Monserud, C. P. Higgins, and J. F. Ranville, *Environmental Toxicology and Chemistry*, 2011, **31**, 115–121.

28. H. E. Pace, N. J. Rogers, C. Jarolimek, V. A. Coleman, E. P. Gray, C. P. Higgins, and J. F. Ranville, *Environmental Science & Technology*, 2012, **46**, 12272–12280.

29. J. Tuoriniemi, G. Cornelis, and M. Hassellöv, *Analytical Chemistry*, 2012, **84**, 3965–3972.

30. S. A. Pergantis, T. L. Jones-Lepp, and E. M. Heithmar, *Analytical Chemistry*, 2012, **84**, 6454–6462.

31. A. K. Brewer and A. M. Striegel, *Analytical and Bioanalytical Chemistry*, 2011, **399**, 1507–1514.

32. G. Lespes and J. Gigault, *Analytica Chimica Acta*, 2011, **692**, 26–41.